Journal of Structural Geology, Vol. 6, No. 4, pp. 425 to 432, 1984
Printed in Great Britain

0191-8141/84 $03.00 + 0.00

Erosion and the mechanics of shallow foreland thrusts

JAMES H. WILLEMIN*

Department of Earth and Planetary Sciences, Massachusetts Institute of Technology, Cambridge, Massachusetts 02139, U.S.A.

(*Received* 5 *July* 1982; *accepted in revised form* 10 *October* 1983)

Abstract—A simple model for the effects of erosion on the geometry and mechanics of shallow foreland thrusts allows prediction of maximum stable length of the thrust toe, location of initial failure within the toe, if total thrust displacement exceeds the maximum stable length, and estimates of average pore fluid pressures along the fault during thrust advance. For 'typical' rates of erosion and thrust advance, the maximum stable length of the toe may be very large (over 50 km) for relatively low values of fluid overpressure. Application of the theoretical results to the Keystone–Muddy Mountain thrust of southern Nevada predicts: maximum stable length, location and degree of imbrication in agreement with observation; relatively low pore fluid pressures along the fault (λ between 0.5 and 0.6), and a rate of thrust advance between 4 and 8 km Ma^{-1}.

INTRODUCTION

EROSION is an important factor in the mechanics of shallow foreland thrusts: by modifying the thickness of the advancing thrust sheet, erosional denudation controls the maximum length of the overriding toe. Thickness of the thrust sheet controls the overburden stress, hence the basal resistance and maximum stable length (e.g. Hubbert & Rubey 1959, Johnson 1981). This work is a quantitative evaluation of the importance of erosion in the mechanics of shallow foreland thrusts.

Earlier work on the significance of erosion in thrusting includes analyses by Raleigh & Griggs (1963) and Johnson (1981). Raleigh & Griggs concluded that in order for thrust advance to occur, erosion must completely remove the advancing toe before significant tectonic overlap develops. Johnson analysed the Keystone–Muddy Mountain thrust of southern Nevada and concluded that a steady-state geometry was attained when the toe reached a length of 25 km. In this paper I present first general relationships between the rate of erosion, rate of thrust advance and the profile of an advancing thrust sheet; I then apply these relationships in a mechanical analysis of the Keystone–Muddy Mountain thrust.

The general theory developed here is particularly relevant to 'erosional thrusts': thrusts whose fault plane was so near the surface of the earth that erosional detritus derived from the advancing allochthon was incorporated into the footwall (Longwell 1949, Davis 1973, Brock & Engelder 1977, Johnson 1981), although a modification of this theory may easily be made for any thrust plate bounded above by an erosional surface during thrust transport. Application of this mechanical development to the Keystone–Muddy Mountain system not only provides an estimate of the maximum stable length of the advancing thrust toe, but also provides an estimate of the stress field near the fault and an estimate of the rate of thrust advance.

* Current address: Department of Geological Sciences, Cornell University, Ithaca, New York 14853, U.S.A.

THEORETICAL DEVELOPMENT

The theory developed here is based on a simple abstraction of an erosional thrust (Fig. 1). I first present a method for estimating the cross-sectional profile of the advancing toe of the thrust sheet, then I analyse the stress field near the base and derive an expression for the mechanical stability (maximum stable length) for such a toe.

Several major assumptions are central to the following development, including the form of the erosion law, the assumed absence of tectonic thickening and a simple frictional fault mechanism. In general, the rate of erosional denudation at a point is a function of slope, climate and bedrock lithology (e.g. Blatt *et al.* 1980). In his analysis of the Keystone thrust of southern Nevada, Johnson (1981) assumed a constant rate of denudation (1 mm a^{-1}). However, studies over a wide range of climatic and lithologic conditions suggest the rate of erosional denudation is proportional to local relief (i.e. slope) (Ahnert 1970, Ruxton & McDougall 1967). The effects of climate and lithology on erosion rate are contained in the constant k in this development: for application to a specific thrust sheet, climate and lithology determine the basic erosion rate, which varies with the changing relief of the advancing thrust toe.

The assumption of no internal thickening is one of the defining axioms of this discussion. In this first-order treatment, there is no attempt to deal with the complications resulting from dynamic thickening of the thrust sheet during advance. Future treatments may include a

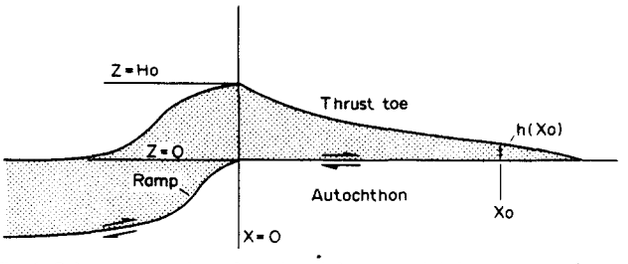

Fig. 1. Schematic section of erosional thrust model showing coordinate system and concave-upward topographic profile.

thickening term, provided some constraints can be placed on the rate and location of profile change due to internal failure, but such complexities are beyond the scope of this simple analysis.

Simple frictional sliding under the influence of possibly elevated pore fluid pressures is perhaps the simplest model for a realistic fault mechanism, and is assumed here not only for the sake of simplicity but also for ease of comparison with previous work (e.g. Hubbert & Rubey 1959, Rubey & Hubbert 1959, Raleigh & Griggs 1963, Johnson 1981, Price & Johnson 1982). Other mechanisms (e.g. flow within a ductile layer or stick-slip) require a straightforward modification of the mechanical discussion and may alter specific conclusions reached regarding pore fluid pressures, stress levels, and so forth, but do not change the fundamental relationships between rate of erosion, rate of thrust advance, profile and overburden stress.

GEOMETRY

The topography developed on an advancing erosional thrust sheet is a result of two competing processes. Denudation removes material and reduces elevation, while tectonic processes such as folding and imbrication tend to thicken the thrust sheet and increase or maintain elevation. For simplicity, it is assumed that changes of shape due to tectonic processes do not occur in the toe of an advancing erosional thrust. Thus the primary process controlling the cross sectional profile is erosion. Assuming that the rate of denudation is proportional to the local relief (Ahnert 1970), I consider two simple cases: the first assumes a completely rigid crust and no isostatic subsidence; the second assumes complete isostatic compensation and zero flexural rigidity for the crust.

Case 1: Rigid crust

Let H_0 be the original thickness of the exposed thrust sheet, $h(x)$ the local thickness (relief), and x the distance away from the top of the ramp (Fig. 1). The rate of denudation is proportional to relief; thus,

$$\frac{dh}{dt} = -kh, \tag{1}$$

where k is a constant with dimension T^{-1}. The sign of k is negative because relief is reduced with time. The thickness h is therefore

$$h = H_0 \exp[-kt], \tag{2}$$

where t is the time a specific point on the upper plate has been exposed to erosion. If r is the average rate of thrust advance, a point on the toe a distance x from the top of the ramp has been exposed to erosion for a time

$$t = x/r. \tag{3}$$

Substituting for t in equation 2, the expression for the thickness of the thrust sheet as a function of distance away from the top of the ramp ($x = 0$) becomes

$$h(x) = H_0 \exp[-(k/r)x]. \tag{4}$$

The ratio of erosion rate constant to rate of thrust advance (k/r) is here defined as the 'profile parameter' α; equation (4) becomes

$$h(x) = H_0 \exp[-\alpha x]. \tag{4a}$$

Case 2: Complete compensation

The second case assumes complete and instantaneous isostatic compensation for the tectonic load of the advancing, eroding thrust sheet, but neglects the effects of any debris wedge or foredeep deposits. Suppose complete isostatic compensation occurs instantaneously, so that the advancing thrust sheet is always in isostatic equilibrium. The local relief $h'(x)$ is now assumed to be that portion of the thrust sheet above the isostatic datum (e.g. sea level), and local relief is related to total thrust sheet thickness $h(x)$ by

$$h'(x) = \left(1 - \frac{\rho t}{\rho m}\right)h(x), \tag{5}$$

where ρ_m is the density of the upper mantle and ρ_t is the density of the advancing thrust sheet. The original differential equation for the rate of denudation then becomes:

$$\frac{dh}{dt} = -kh' \tag{6}$$

$$= -k(1 - \rho_t/\rho_m)h, \tag{6a}$$

and the expression for the thickness of the thrust sheet at some distance x away from the top of the ramp becomes:

$$h(x) = H_0 \exp\left\{-\left(\frac{k(1 - \rho t/\rho m)}{r}\right)x\right\}$$

$$= H_0 \exp(-\alpha(1 - \rho_t/\rho_m)x). \tag{7}$$

The effect of subsidence is to lessen the influence of erosion in reducing the thickness of the advancing thrust toe. That is, complete isostatic compensation will reduce the profile parameter α by a factor of ρ_t/ρ_m. The significance of this potential reduction of α on the mechanical stability of the advancing thrust sheet will become apparent in the next section.

MECHANICS

By removing material from an advancing thrust sheet, erosion reduces the thickness and cross-sectional area of the thrust sheet. Reducing thickness reduces the vertical stress, thus reducing fault zone resistance according to Coulomb's law:

$$\tau = \mu\sigma_n + C, \tag{8}$$

where τ is the shear strength of the fault, σ_n is the normal stress across the fault, μ is the coefficient of friction and C is the cohesive strength of the fault. Reducing cross sectional area reduces the strength of the thrust sheet, hence the ability of the thrust sheet as a whole to

overcome the fault zone resistance. Thus, the overall effect of erosional denudation on thrust mechanics is the result of two contrasting principles: reduction of resistance and reduction of strength.

The relative importance of these two contrary effects is determined primarily by the profile of the thrust sheet for a given lithology and fault mechanism. In the following discussion, the thrust sheet is assumed to consist of rocks with uniform lithology obeying the Mohr–Coulomb failure criterion (Jaeger & Cook 1976). The fault mechanism is assumed to be simple sliding friction. Under these assumptions calculation of maximum stable length of the thrust toe serves as a simple gauge of the relative importance of the two effects of erosion: a high maximum stable length suggests reduction of resistance is dominant, while a low maximum stable length suggests reduction of strength is the most important effect of erosion.

Fault zone resistance

For a subhorizontal fault with simple frictional sliding mechanism, the fault zone resistance at a point x is a function of fault zone depth and pore fluid pressure (Hubbert & Rubey 1959)

$$\tau = \mu(\rho g z)(1 - \lambda_f) + C, \tag{9}$$

where τ is the fault zone resistance, μ is the coefficient of friction, g is the acceleration of gravity, z is the depth of the fault, λ_f is the ratio of pore fluid pressure to vertical stress within the fault zone and C is the cohesive strength of the fault. For stable sliding, cohesive strength is assumed to vanish and the coefficient of friction is assumed to lie between 0.6 and 0.75 (Dieterich 1979). If the fault zone material is relatively impermeable, lateral changes in λ_f should be relatively small; therefore λ_f will be assumed constant. Thus, the fault zone resistance is a function of position on the eroding toe

$$\tau = \mu\rho g(1 - \lambda_f)h(x). \tag{10}$$

Following Hubbert and Rubey (1959), the average horizontal stress σ_h^* at a point x required to overcome fault zone resistance is

$$\sigma_h^*(x) \cdot h(x) = \int_x^{x_t} \tau(u)\,du, \tag{11}$$

where x_t is the position of the leading edge of the advancing toe. Substituting for τ and $h(x)$ from eqns. 4(a) and 9, the expression for σ_h^* becomes:

$$\begin{aligned}\sigma_h^*(x) &= (H_0 \exp(-\alpha_x))^{-1}\mu\rho g(1 - \lambda_f)H_0 \int \exp(-\alpha x)\,dx \\ &= \mu\rho g(1 - \lambda_f)(1/\alpha)(1 - \exp(-\alpha(x_t - x))).\end{aligned} \tag{12}$$

In the (hypothetical) absence of pore fluids within the body of the thrust sheet, the horizontal stress σ_h at the base of the sheet, here taken as twice the average horizontal stress, is

$$\sigma_h = (2\mu\rho g/\alpha)(1 - \lambda_f)(1 - \exp(-\alpha(x_t - x))), \tag{13a}$$

the vertical stress at the base of the sheet is

$$\sigma_v = \rho g H_0 \exp(-\alpha x), \tag{13b}$$

and the shear stress at the base is

$$\tau = \mu\rho g H_0(1 - \lambda_f)\exp(-\alpha x). \tag{13c}$$

If pore fluids are present within the body of the thrust sheet, the effective vertical and horizontal stresses are

$$\sigma_h' = (1 - \lambda_b)(2\mu\rho g/\alpha)(1 - \lambda_f)(1 - \exp(-\alpha(x_t - x))) \tag{13d}$$

and

$$\sigma_v' = (1 - \lambda_b)\rho g H_0 \exp(-\alpha x), \tag{13e}$$

where λ_b is the ratio of pore fluid pressure within the body of the thrust sheet to vertical stress. If the fault zone permeability differs greatly from that of the surrounding rock, λ_b may be much different than λ_f. The ratio of horizontal to vertical effective stresses near the base of an advancing erosional thrust toe is obtained by dividing eqn. 13(d) by eqn. 13(e):

$$\frac{\sigma_h}{\sigma_v} = \frac{\sigma_h'}{\sigma_v'} = \frac{2\mu(1 - \lambda_f)}{\alpha H_0}\exp(\alpha x)(1 - \exp(-\alpha(x_t - x))). \tag{14}$$

Thus, the ratio of horizontal to vertical stress varies with position along the thrust toe (Appendix). Indeed, the Differentiating (14) with respect to x, the stress ratio σ_h/σ_v attains a maximum at the point

$$x = x_t - (\log_e 2)/\alpha. \tag{15}$$

The maximum value of the stress ratio is:

$$(\sigma_h/\sigma_v)_{max} = (\mu(1 - \lambda_f)/2\alpha H_0)\exp(\alpha x_t). \tag{16}$$

The state of stress on the fault plane is completely determined by σ_h, σ_v and τ (Jaeger 1969). The principal stress inclination is defined by the angle θ between σ_1 and σ_h, given by (Jaeger 1969, p. 7)

$$\theta = 1/2 \tan^{-1}(2\tau/(\sigma_h - \sigma_v)) \tag{17a}$$

and the principal stress magnitudes are given by

$$\sigma_1 = 1/2(\sigma_h + \sigma_v + (\sigma_h - \sigma_v)/\cos(2\theta)) \tag{17b}$$

$$\sigma_3 = 1/2(\sigma_h + \sigma_v - (\sigma_h - \sigma_v)/\cos(2\theta)), \tag{17c}$$

where θ is as above.

Substituting for σ_h, σ_v and τ from equations (13), it follows that the principal stress inclination θ and the ratio of principal stress magnitudes σ_1/σ_3 vary with position along the thrust toe (Appendix). Indeed, the principal stress ratio is greatest and the principal stresses most nearly parallel to σ_h and σ_v (θ smallest) at the point where σ_h/σ_v is maximum

$$x_0 = x_t - (\log_e 2)/\alpha. \tag{18}$$

Strength

The preceding section developed a formalism for calculation of the stress field near the base of a hypothetical erosional thrust toe, assuming no internal thickening. In this section, a set of relations is developed to predict the onset of imbrication within the advancing

thrust toe as a function of the length and thickness of the advancing thrust sheet, the profile parameter α and the pore fluid pressure both within the body of the thrust sheet and within the fault zone. The resulting equations allow the prediction of the location of the primary imbrications within an advancing erosional thrust.

Mechanical failure of a body (in this case imbrication of the erosional thrust sheet) occurs when the stresses within the body exceed the strength, specified by a failure criterion. Choice of a failure criterion for a thrust sheet depends on lithology, pre-existing structure or weakness, rate of deformation and the physical conditions of deformation (pressure, temperature, etc.). For this study I assume that the toe of the advancing thrust sheet is pervasively fractured, with potential slip surfaces existing in all orientations, and that failure will occur when the shear stress on the most favorably oriented of these surfaces exceeds the static friction.

For most rocks at confining pressures below 200 MPa, Byerlee (1978) found that static friction on a fracture could be described by a form of the Mohr–Coulomb failure criterion

$$\tau = \xi(\sigma_n - P_f), \tag{19}$$

where τ and σ_n are the shear and normal stresses on the fracture, P_f is the pore fluid pressure and ξ is the coefficient of static friction. Byerlee found that for most rocks $\xi = 0.85$, regardless of lithology (excepting certain clays). This relation can be re-cast in terms of the principal stresses σ_1 and σ_3 (Jaeger 1969, p. 76)

$$\frac{\sigma_1}{\sigma_3} = \frac{(\xi + (\xi^2 + 1)^{1/2} - 2\xi(P_f - C_0)/\sigma_3)}{(\xi^2 + 1)^{1/2} - \xi} \tag{20}$$

or, letting $\xi = 0.85$ and $C_0 = 0$,

$$\sigma_1/\sigma_3 = 4.7 - 3.67(P_f/\sigma_3). \tag{21}$$

Failure of the thrust sheet will occur first where the ratio σ_1/σ_3 is largest. It was stated above that σ_1/σ_3 attains a maximum and that the principal stress directions are most nearly horizontal and vertical at the point $x_0 = x_t - \log_e 2)/\alpha$. Approximating σ_1 by σ_h and σ_3 by σ_v, the failure condition for the thrust sheet becomes:

$$\sigma_h/\sigma_v = 4.7 - 3.67(P_f/\sigma_v) \tag{21a}$$

or, from equation (16),

$$(\mu(1 - \lambda_f)/2\alpha H_0) \exp(\alpha x_t) = 4.7 - 3.67\lambda_b. \tag{22}$$

The ratio P_f/σ_v is λ_b, equivalent to the parameter λ defined by Hubbert & Rubey (1959) for the region within the body of the thrust sheet and possibly distinct from λ_f defined above. Solving for $x_{t\,max}$, the maximum stable length, the failure condition can be written;

$$x_{t\,max} = (1/\alpha) \log_e ((4.7 - 3.67\lambda_b)2\alpha H_0/(\mu(1 - \lambda_f))). \tag{23}$$

Thus, when the distance between the leading edge and the top of the ramp reaches $x_{t\,max}$ an imbricate fault will form within the toe of the thrust sheet at a distance $(\log_e 2)/\alpha$ from the leading edge (Fig. 2).

During the early stages of thrust advance, the distance

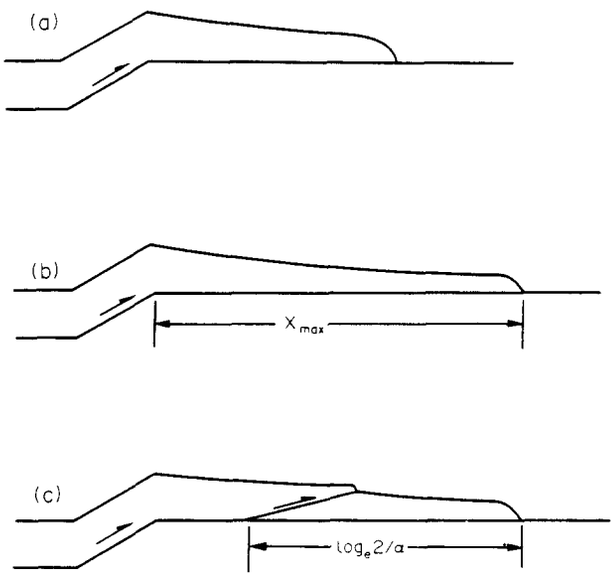

Fig. 2. Structural history of an advancing erosional thrust toe: (a) Total displacement less than maximum stable length. The toe remains coherent without internal thickening. (b) Total displacement equals maximum stable length. The thrust toe becomes mechanically unstable with further displacement on the main thrust. (c) Total displacement greater than maximum stable length. An imbrication has formed at the point of greatest principal stress ratio and internal thickening becomes mechanically important.

x_t between the leading edge of the thrust toe and the top of the ramp will be small ($x_t < (\log_e 2)/\alpha$), and this analysis will not hold. In this case, the maximum principal stress ratio and minimum principal stress inclination will occur at the top of the ramp ($x = 0$). It is possible that the thrust sheet will become mechanically unstable during this early phase, while $x_t < \log_e 2/\alpha$. Again assuming that $\sigma_1 \approx \sigma_h$ and $\sigma_3 \approx \sigma_v$ and that failure will occur according to equation (21), imbrication will occur at the top of the ramp ($x = 0$) if

$$\begin{aligned}\sigma_h/\sigma_v &= (2\mu(1 - \lambda_f)/\alpha H_0)(1 - \exp(-\alpha x_t)) \\ &= 4.7 - 3.67\lambda_b.\end{aligned} \tag{24}$$

Solving for x_t, imbrication at the top of the ramp will occur if

$$\begin{aligned}(\log_e 2)/\alpha &> x_t \\ &= -(1/\alpha) \log_2 (1 - (\alpha H_0/2\mu(1 - \lambda_f))(4.7 - 3.67\lambda_b))\end{aligned}$$

or

$$1/2 > (\alpha H_0/2\mu(1 - \lambda_f))(4.7 - 3.67\lambda_b). \tag{25}$$

Thus, imbrication at the top of the ramp will occur if the toe is thin, friction high, erosion slow, or if excess pore fluid pressure weakens the thrust sheet (λ_b high).

In this section the stress field near the base of an advancing erosional thrust toe has been determined as a function of basal friction μ, total toe length x_t and 'profile parameter' α. From the expressions derived for the principal stresses, it was determined that the advancing thrust sheet will first become mechanically unstable (begin internal thickening) at a point that may be some distance from both the leading edge and the top of the ramp. In the next sections, I first discuss these various expressions, then apply the formalism developed here to

a classic example of a real erosional thrust: the Keystone–Muddy Mountain thrust system of southern Nevada (Longwell 1949, Davis 1973, Burchfiel *et al.* 1974, Willemin *et al.* 1981, Johnson 1981, Price & Johnson 1982).

DISCUSSION

Perhaps the single most important parameter in this development is the 'profile parameter' α. Defined as the ratio of erosion rate constant to the rate of thrust advance, α is a measure of the taper of the erosional wedge. Large values of α mean that the rate of erosion is relatively large, and that the geometry of the advancing thrust sheet is strongly altered by erosional denudation, while smaller values of α indicate that thrust advance is fast with respect to erosion and the profile of the thrust sheet is relatively little altered by erosion. The influence of this parameter can be seen in the expression for the location of the maximum principal stress ratio (eqn 18):

$$x_0 = x_t - (\log_e 2)/\alpha.$$

For large values of α (steep taper), the maximum principal stress ratio occurs near the leading edge of the toe, while for small values of α (gentle taper) the maximum principal stress ratio occurs closer to the back of the advancing toe. Thus, α controls the relative position of the first internal imbrication of the thrust wedge: a quickly eroding thrust sheet will fail near the leading edge, while a slowly eroding thrust toe will fail nearer the top of the ramp.

This is also apparent in the expression for the maximum stable length, (eqn 23):

$$x_{t\,max} = (1/\alpha)\log_e((4.7 - 3.67\lambda_b)2\alpha H_0/(\mu(1-\lambda_f))).$$

Thus, for large values of α, denoting rapid erosion and steep taper, the maximum stable length is smaller (imbrication occurs nearer the leading edge) than for smaller values of α. That is, rapid erosion tends to reduce the strength of the thrust sheet faster than reducing the fault zone resistance. The effect of subsidence (isostatic compensation) is to reduce the value of α; thus, rapid subsidence under tectonic loading would tend to increase the maximum stable length of the thrust toe.

Another important aspect of this treatment is the separation of the effects of pore fluid pressures within the body of the thrust sheet and within the fault zone at the base. These two factors have contrary effects on the mechanical stability of the thrust sheet: as pore fluid pressure within the fault zone increases (λ_f increases), the fault zone resistance decreases and the maximum stable length increases, as predicted by Hubbert & Rubey (1959). However, as the pore fluid pressure within the body of the thrust sheet increases (λ_b increases) the strength of the thrust sheet is reduced and the maximum stable length decreases (eqn. 25). The relative importance of λ_f and λ_b are illustrated in Fig. 3, showing the maximum stable length of a hypothetical erosional thrust toe as a function of λ_f and λ_b, calculated for a 'typical' (arbitrary) profile parameter α and initial thickness H_0.

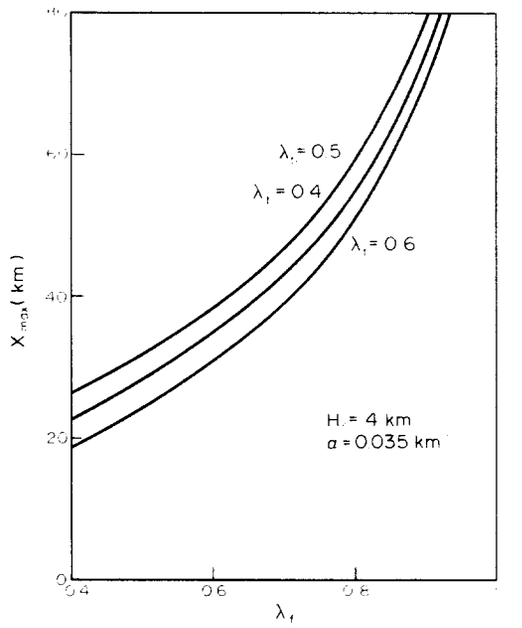

Fig. 3. Maximum stable length of a thrust toe as a function of pore pressure-to-overburden ratio in the fault zone (λ_f) and within the thrust sheet (λ_b). Rate of thrust advance 5 km Ma^{-1}, maximum rate of erosion 0.7 mm a^{-1}.

In this section it has been shown how erosion of the upper plate modifies the mechanics of transport of the toe of an erosional thrust, including stress levels and orientations and maximum tectonic overlap prior to internal imbrication. In the next section, the relationships developed here are applied to the Keystone–Muddy Mountain thrust system of southern Nevada, and the results compared with those of a previous analysis by Price & Johnson (1982).

APPLICATION TO THE KEYSTONE–MUDDY MOUNTAIN THRUST SYSTEM

The Keystone–Muddy Mountain thrust system of southern Nevada and southeastern California is one of the 'type' erosional thrusts of the North American Cordillera (e.g. Longwell 1949, 1960, Burchfiel *et al.* 1974, Burchfiel & Davis 1971, Brock & Engelder 1977, Carr 1980, Burchfiel *et al.* 1981, Price & Johnson 1982). The Keystone–Muddy Mountain thrust system represents the frontal foreland thrust of the Sevier (Late Cretaceous) orogenic event.

Recent structural studies define three broad provinces within the Keystone–Muddy Mountain thrust system: the Muddy Mountains province, where the Keystone–Muddy Mountain thrust forms an erosional toe; the central Spring Mountains province, where the Keystone–Muddy Mountain thrust system either rides at depth or is ramping to the surface; and the southern Spring Mountains province, where the Keystone–Muddy Mountain thrust system again forms an erosional toe (Burchfiel *et al.* 1974, Willemin *et al.* 1981, Bohannon 1981). Data from all three provinces are used in this example.

Information from the Muddy Mountains can be used to determine the profile parameter α for the toe of the Keystone–Muddy Mountains system. Recent mapping by Bohannon (1981) shows an upper plate thickness of at least 1800 meters is presently preserved in the eastern part of the Muddy Mountains. This thickness represents an absolute minimum, because the upper plate rocks were exposed to erosion for an extended period between the cessation of thrusting in the late Cretaceous (Fleck 1970) and final burial by Miocene sediments (Bohannon 1981). Considering this period of erosion, I will assume that at the cessation of thrusting the upper plate in the eastern Muddy Mountains was not less than 2 km thick. Palinspastic restoration of Tertiary deformation indicates that this thickness occurs at least 20 km from the top of the ramp (Bohannon 1981).

In the central province, the Keystone thrust sheet is between 4 and 5 km thick as it ramps to the surface (Burchfiel *et al.* 1974). I assume that the Keystone–Muddy Mountain thrust sheet was about 4 km thick at the top of the ramp. Thus, from an initial thickness of 4 km, the Keystone–Muddy Mountain thrust sheet had been eroded to a thickness of 2 km after advancing 20 km. The profile parameter α is given by the relation

$$\alpha = -(1/x)\log_e(h(x)/H_0)$$

or, for the Keystone–Muddy Mountain thrust,

$$\alpha = -(1/20)\log_e(2/4)$$
$$= 0.0347\ \text{km}^{-1}.$$

It is now possible to estimate the maximum stable length of the toe of the Keystone–Muddy Mountain thrust system using eqn (23). Assuming values of $\mu = 0.6$ and $\lambda_b = 0.4$ (hydrostatic equilibrium), the values for H_0 and α above provide an expression for the maximum stable length of the Keystone–Muddy Mountain thrust toe as a function of λ_f:

$$x_{max} = 28.9\log_e(1.49/(1-\lambda_f)).$$

Values of x_{max} for various choices of λ_f and λ_b are given in Table 1. Price & Johnson (1982) suggest a value of λ_f between 0.6 and 0.8; these estimates yield a maximum stable length between 38 and 58 km.

A check of this prediction can be made by estimating the maximum stable length of the toe from field observations. In the central Spring Mountains province the Keystone–Muddy Mountain thrust sheet shows little imbrication and internal deformation as it ramps to the surface (Burchfiel *et al.* 1974). Mapping by Bohannon (1981) in the Muddy Mountains province shows a series of imbricate slices within the toe. This suggests that failure occurred within the toe, resulting in imbrication. Thus the total displacement on the Keystone–Muddy Mountain thrust exceeded the maximum stable length of the toe.

Mismatch of upper and lower plate features on the Keystone–Muddy Mountain thrust suggest a minimum total displacement of 40 to 50 km (Burchfiel *et al.* 1981, 1982, Willemin *et al.* 1981). If the internal deformation in the toe requires that the total displacement significantly exceeds the maximum stable length of the toe, then the maximum stable length must be less than 40–50 km. This in turn suggests that the average pore fluid pressures within the fault zone were somewhat less than suggested by Price & Johnson (1982). It is of interest to note that of the imbricate faults mapped by Bohannon (1981), none are observed to splay off of the basal thrust within the 20 km length exposed, in agreement with the calculations here.

Table 1. Maximum stable length for the toe of the Keystone–Muddy Mountain thrust system

	λ_f					
λ_b	0.4	0.5	0.6	0.7	0.8	0.9
0.4	26.3	31.5	38.0	46.0	58.0	78.0
0.5	22.8	28.0	34.5	42.8	54.5	74.5
0.6	(18.9)	24.1	30.6	38.9	50.5	70.5
0.7	(14.3)	(19.6)	26.0	34.3	46.0	66.0
			x_{max} (km)			

In addition to predicting the maximum stable length, the profile parameter α may be used to obtain a first-order estimate of the rate of thrust advance by assuming an erosional rate constant. In a global study of large mid-latitude drainage basins, Ahnert (1970) inferred an erosional rate constant $k = 0.1545\ \text{Ma}^{-1}$; this would correspond to a maximum rate of denudation of 0.6 mm a^{-1} at the top of the ramp for the Keystone–Muddy Mountain system. Johnson (1981) assumed a constant rate of erosion of 1 mm a^{-1}; this would correspond to an erosional rate constant $k = 0.25\ \text{Ma}^{-1}$. Assuming a rigid crust, the rate of thrust advance is simply k/α; thus using Ahnert's estimate for k, the average rate of thrust advance for the Keystone–Muddy Mountain system is

$$r = 0.1545\ \text{Ma}^{-1}/0.0347\ \text{km}^{-1} = 4.5\ \text{km Ma}^{-1}$$

while using Johnson's estimate,

$$r = 0.25\ \text{Ma}^{-1}/0.0347\ \text{km}^{-1} = 7.7\ \text{km Ma}^{-1}.$$

If complete and instantaneous isostatic compensation occurred during thrusting, the average rate of thrust advance would be given by (eqn. 7)

$$r = (1-\rho_t/\rho_m)k/\alpha. \qquad (26)$$

Assuming $\rho_t = 2.5$ and $\rho_m = 3.3\ \text{gm cm}^{-3}$, the estimated rates of thrust advance become $r = 1.1\ \text{km Ma}^{-1}$ for Ahnert's erosion rate constant and $r = 1.7\ \text{km Ma}^{-1}$ using Johnson's rate constant.

The rates calculated assuming a rigid crust are within the range allowed by available age controls (Fleck 1970, Burchfiel & Davis 1971, 1977, Carr 1980), while the rates calculated assuming complete isostatic compensation appear to be somewhat too slow. This result suggests that either erosion was more rapid than estimated here (by roughly a factor of 4) or that isostatic compensation did not occur on the time scale of thrust emplacement. The latter possibility is supported by the lack of foredeep sediments preserved in the Keystone–Muddy Mountain foreland (e.g. Longwell *et al.* 1965).

CONCLUSIONS

Proceeding from an assumption that the rate of erosion is proportional to relief, it has been shown how rapid erosion or a rigid crust reduces the mechanical stability of an advancing erosional thrust, while relatively slow erosion or rapid isostatic compensation tends to increase the mechanical stability of an erosional thrust. In effect, this means that erosional denudation tends to reduce the strength of an advancing thrust toe faster than reducing fault zone resistance. Calculation of the stress field near the base of the thrust sheet shows that the ratio of principal stresses attains a maximum and the inclination of principal stresses attains a minimum at a constant distance from the leading edge of the advancing thrust sheet: $x = x_t - (\log_e 2)/\alpha$; this point has been used to calculate the maximum stable length of an erosional thrust toe.

Application of the theory developed here to the Keystone–Muddy Mountain thrust system of southern Nevada yields results entirely compatible with observation: imbrication began near the top of the ramp as total displacement began to exceed the maximum stable length of the toe, which was around 25–30 km. Probable rates of thrust advance, obtained from the profile parameter and estimates of erosion rate constants, lie between 4 and 8 km Ma^{-1}. The average horizontal stress at the top of the ramp just before imbrication was probably on the order of 200 MPa, assuming hydrostatic pore fluid pressures.

Although this development has been restricted to a small segment of a thrust belt, it illustrates again the importance of erosion and topography in modifying the stress field during thrusting (Elliott 1976) and also illustrates the possible significance of non-linear topographic profiles on the stress field.

Acknowledgements—This work is one result of a continuing study of the tectonics of the southwestern U.S. being directed by B. C. Burchfiel and G. A. Davis. W. Royden, D. Walker, K. Hodges, B. Wernicke and L. Serpa provided valuable input throughout the progress of this paper. The research was supported by the National Science Foundation through grant EAR 77-13637 to B. C. Burchfiel, the author's advisor at MIT.

REFERENCES

Ahnert, F. 1970. Functional relationship between denudation, relief and uplift in large drainage basins. *Am. J. Sci.* **268**, 243–263.

Blatt, H., Middleton, G. & Murray, R. 1980. *Origin of Sedimentary Rocks* (2nd. ed.). Prentice Hall, Englewood Cliffs, New Jersey.

Bohannon, R. 1981. Geologic map, tectonic map and structure sections of the Muddy and northern Black Mountains, Clark County, Nevada. U.S. Geological Survey Open File Report OF 81-796, 3 sheets.

Brock, W. G. & Engelder, T. 1977. Deformation associated with movement of the Muddy Mountain overthrust in the Buffington window, southeastern Nevada. *Bull. geol. Soc. Am.* **88**, 1667–1677.

Burchfiel, B. C. & Davis, G. A. 1971. Clark Mountain thrust complex in the Cordillera of southeastern California: geologic summary and field trip guide. *California Univ. Riverside, Campus Mus. Contr.* **1**, 1–28.

Burchfiel, B. C., Fleck, R. J., Secor, D. T., Vincelette, R. R. & Davis, G. A. 1974. Geology of the Spring Mountains, Nevada. *Bull. geol. Soc. Am.* **85**, 1013–1022.

Burchfiel, B. C., Wernicke, B., Willemin, J. H., Cameron, C. S., Axen, G. J. & Davis, G. A. 1982. A new type of decollement thrusting. *Nature, Lond.* **300**, 513–515.

Burchfiel, B. C., Willemin, J. H., Carr, M. D., Cameron, C. S., Axen, G. J. & Davis, G. A. 1981. Style and geometry of thrusting and related deformation, Keystone thrust system, southern Nevada and southeastern California. *Geol. Soc. Am. Abs. with Progms* **13** (7), 419.

Byerlee, J. D. 1978. Friction of Rocks. *Pure appl. Geophys.* **116**, 615–626.

Carr, M. D. 1980. Upper Jurassic to lower Cretaceous (?) synorogenic sedimentary rocks in the southern Spring Mountains, Nevada. *Geology* **8**, 385–390.

Davis, G. A. 1973. Relations between the Keystone and Red Spring thrust faults, eastern Spring Mountains, Nevada. *Bull. geol. Soc. Am.* **84**, 3709–3716.

Dieterich, J. H. 1979. Modeling of rock friction, 1, Experimental results and constitutive equations. *J. geophys. Res.* **84**, 2161–2169.

Elliott, D. 1976. Motion of thrust sheets. *J. geophys. Res.* **81**, 949–963.

Fleck, R. J. 1970. Tectonic style, magnitude and age of deformation in the Sevier orogenic belt in southern Nevada and eastern California. *Bull. geol. Soc. Am.* **81**, 1705–1720.

Hubbert, M. K. & Rubey, W. 1959. Role of fluid pressure in overthrust faulting. *Bull. geol. Soc. Am.* **70**, 115–166.

Jaeger, J. C. 1969. *Elasticity, Fracture and Flow*. Chapman & Hall, London.

Jaeger, J. C. & Cook, N. G. W. 1976. *Fundamentals of Rock Mechanics* (2nd ed.). Chapman Hall, London.

Johnson, M. R. W. 1981. The erosion factor in the emplacement of the Keystone thrust sheet (south east Nevada) across a land surface. *Geol. Mag.* **118**, 501–507.

Longwell, C. R. 1949. Structure of the northern Muddy Mountain area, Nevada. *Bull. geol. Soc. Am.* **60**, 923–967.

Longwell, C. R. 1960. Possible explanation of diverse structural patterns in southern Nevada. *Am. J. Sci.* **258A**, 192–203.

Longwell, C. R. 1973. Structural studies in southern Nevada and western Arizona: a correction. *Bull. geol. Soc. Am.* **84**, 3717–3720.

Longwell, C. R., Pampeyan, E. H., Bowyer, B. & Roberts, R. J. 1965. Geology and mineral deposits of Clark County, Nevada. *Nevada Bureau Mines Geol. Bull.* **62**.

Price, N. J. & Johnson, M. R. W. 1982. A mechanical analysis of the Keystone–Muddy Mountain thrust in southeast Nevada. *Tectonophysics* **84**, 131–150.

Raleigh, C. B. & Griggs, D. T. 1963. Effect of the toe in the mechanics of overthrust faulting. *Bull. geol. Soc. Am.* **74**, 819–830.

Rubey, W. W. & Hubbert, M. K. 1959. Role of fluid pressure in overthrust faulting: II, Overthrust belt in geosynclinal area of western Wyoming in light of fluid pressure hypothesis. *Bull. geol. Soc. Am.* **70**, 167–205.

Ruxton, B. P. & McDougall, I. 1967. Denudation rates for northeast Papua from potassium–argon dating of lavas. *Am. J. Sci.* **265**, 545–561.

Willemin, J. H., Burchfiel, B. C., Carr, M. D., Axen, G. J., Cameron, C. S. & Davis, G. A. 1981. Detailed geometry of a foreland thrust: the Keystone, thrust, southern Nevada and eastern California. *Geol. Soc. Am. Abs. with Progms* **13** (7), 581.

APPENDIX

Derivation of point of maximum principal stress ratio. (1) Point of minimum principal stress inclination θ:

From equation (17), $\theta = 1/2 \arctan (2\tau/\sigma_h - \sigma_v)$. Substituting for τ from (10) and factoring σ_v,

$$\theta = 1/2 \arctan (2\mu(1 - \lambda_f)/(\sigma_h/\sigma_v) - 1). \quad \text{(A1)}$$

From calculus,

$$\frac{d}{dx}(\arctan (u)) = \frac{1}{1 + u^2}\frac{du}{dx}.$$

Therefore, $d\theta/dx = 0$ if $d/dx(2\mu(1 - \lambda_f)/(\sigma_h/\sigma_v) - 1) = 0$. From (14),

$$\frac{2\mu(1 - \lambda_f)}{(\sigma_h\sigma_v) - 1} = \frac{2\mu(1 - \lambda_f)}{(2\mu/\alpha H_0)(1 - \lambda_f)\exp(\alpha x)(1 - \exp(-\alpha(x_t - x))) - 1}. \quad \text{(A2)}$$

Differentiating the right hand side with respect to x, (A2) becomes

$$\frac{-((2\mu(1-\lambda_f))^2/H_0)(\exp(\alpha x) - 2\exp(-\alpha(x_t - 2x)))}{((2\mu/\alpha H_0)(1-\lambda_f)\exp(\alpha x)(1-\exp(-\alpha(x_t - x))) - 1)^2}. \quad \text{(A3)}$$

The expression (A3) vanishes when

$$\exp(\alpha x) - 2\exp(-\alpha(x_t - 2x)) = 0$$

or

$$x = x_t - (\log_e 2)/\alpha.$$

(2) Point of maximum principal stress ratio.

Let $A = \sigma_h/\sigma_v$. Then from equations (17),

$$\frac{\sigma_1}{\sigma_3} = \frac{(A+1) + (A-1)\cos 2\theta}{(A+1) + (A-1)\cos 2\theta}. \quad \text{(A4)}$$

If A' and θ' represent the derivatives of A and θ with respect to x, then both A' and θ' vanish when $x = x_t - (\log_e 2)/\alpha$. Differentiating (A4) with respect to x.

$$\frac{d}{dx}\frac{\sigma_1}{\sigma_3} = \left(\frac{((A+1)-(A-1)\cos 2\theta)(A' + A'\cos 2\theta - ((A-1)\sin 2\theta)\theta')}{((A+1) - (A-1)\cos 2\theta)^2}\right) - \left(\frac{((A+1)+(A-1)\cos 2\theta)(A' - A'\cos 2\theta + ((A-1)\sin 2\theta)\theta')}{((A+1) - (A-1)\cos 2\theta)^2}\right). \quad \text{(A5)}$$

Because A' and θ' equal 0 at the same point x, the numerator on the right hand side of (A5) becomes 0 when $x = x_t - (\log_e 2)/\alpha$. Simple numerical calculations show that the principal stress ratio is a maximum rather than a minimum at this point. QED.